Supplementary Information for

4D printing of architected metal structures via biodegradation

Yu Qin et al.

Contents

Supplementary Note 1: Printing of 4DAMS

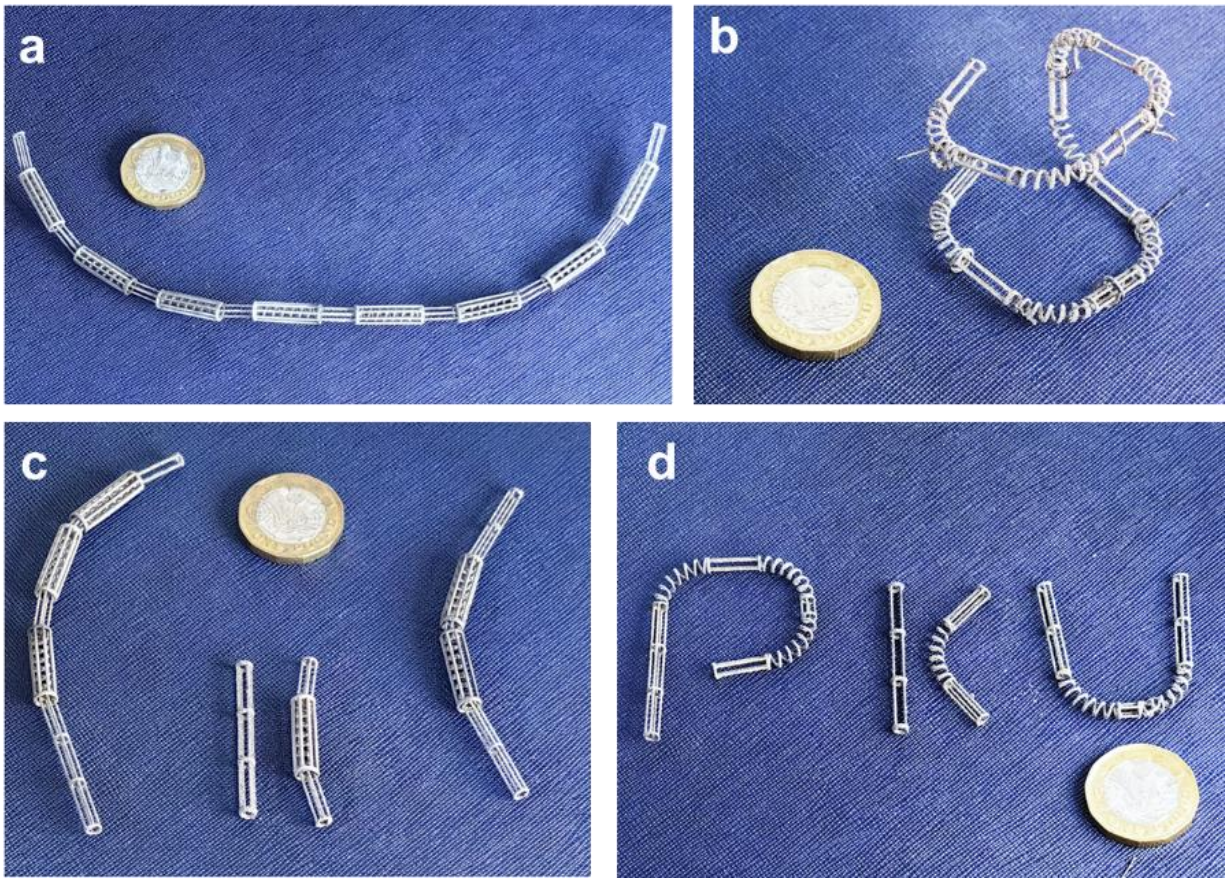

Fig. S1 Bending-type 4DAMS before and after immersion in Hank's solution. a and **b** Recovery of 3D structure. **c** and **d** Recovery of 2D structure.

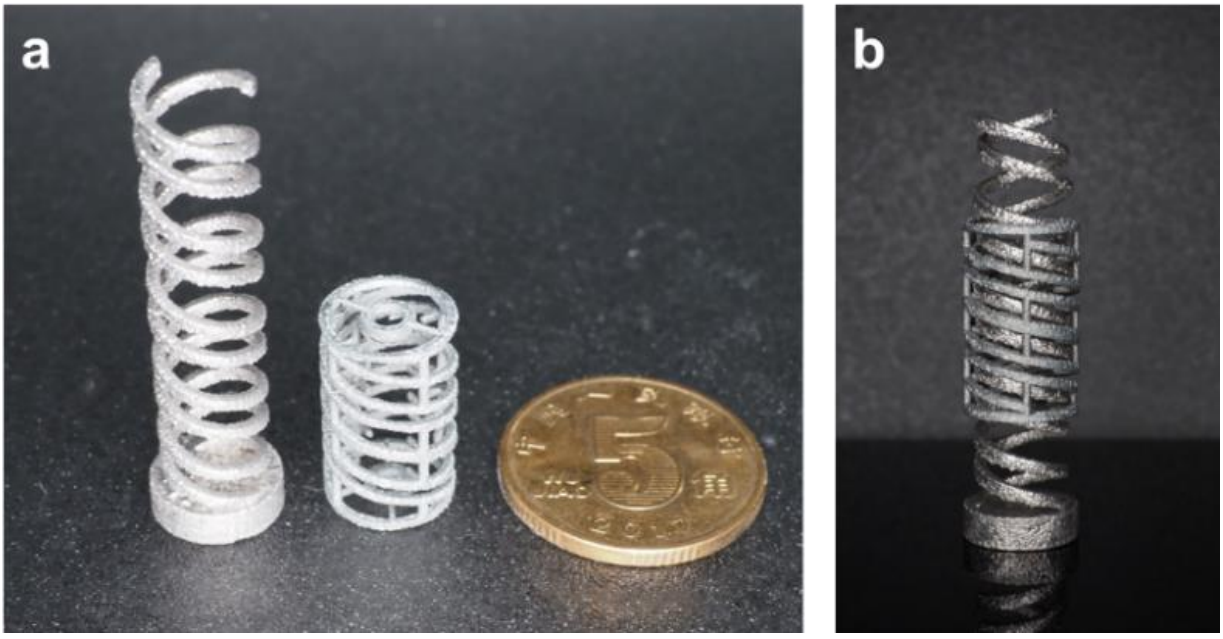

Fig. S2 As-built samples of stretching-type 4DAMS. a Mg spring constraint and Zn scaffold. **b** Assembly of Zn@Mg 4DAMS.

Supplementary Note 2: Characterization of stretching-type 4DAMS

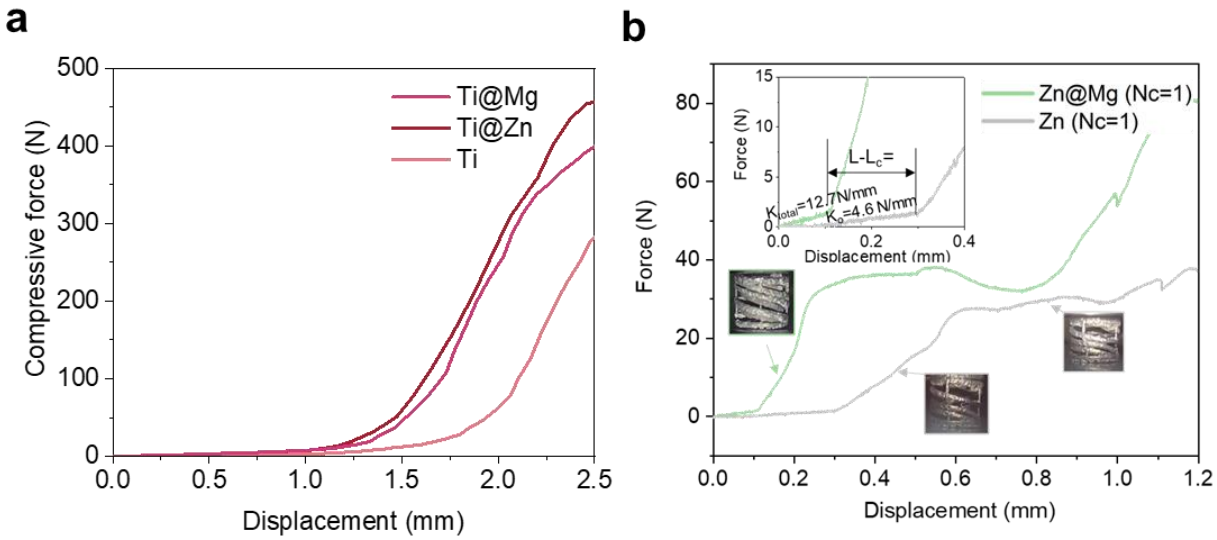

Fig. S3 Compression properties with different design parameters. a Compression curves of Ti, Ti@Zn, and Ti@Mg scaffolds. **b** Compression curves of Zn and Zn@Mg when $N_c = 1$.

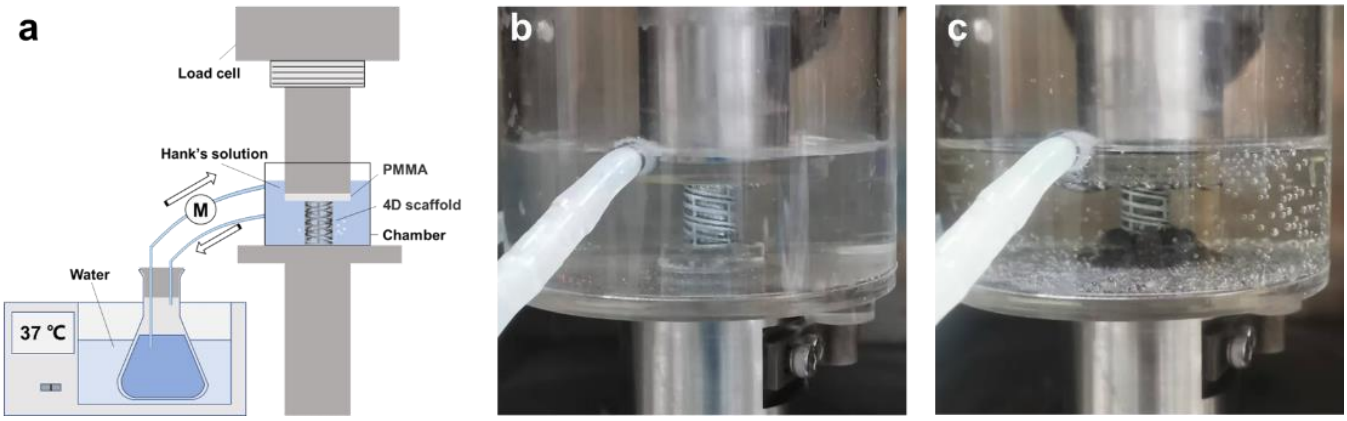

Fig. S4 Recoil force testing. a Schematic of experiment establishment. **b** Immersion of Zn@Mg 4DAMS at 0 h and **c** at 48 h.

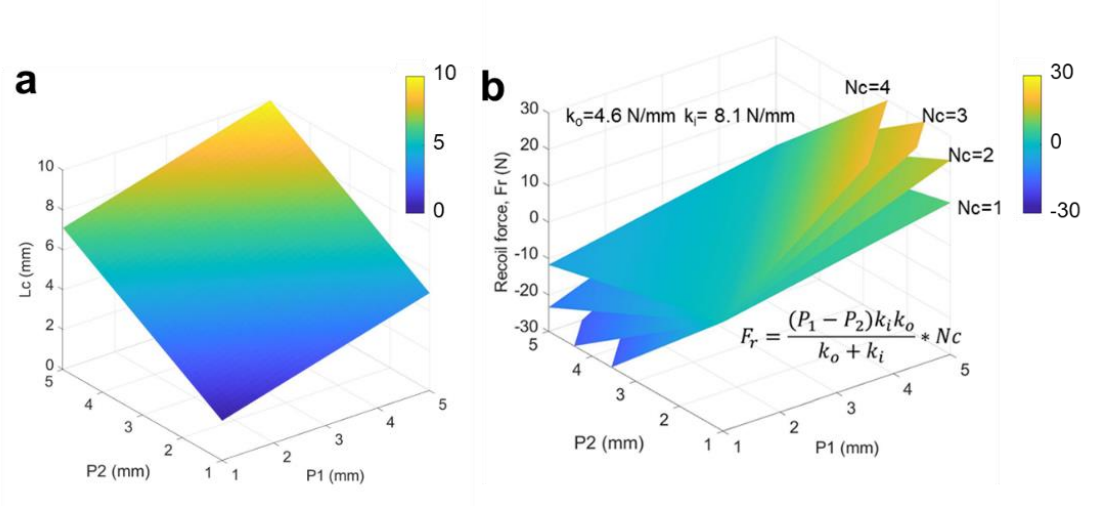

Fig. S5 Theoretical calculation of mechanical propterties with different design parameters. a Compressed length (L-L_c). **b** Recoil force with varying N_c.

Table. S1 Comparison of experimental results with theoretical calculations

P1-P2=0.6	ko(N/mm)	ki(N/mm)	Fr.exp (N)	Fr.theo (N)	Lc-L.exp (mm)	Lc-L.theo (mm)
Zn@Mg	1.5±0.2	3.9±0.2	1.3±0.3	1.3	0.91±0.05	0.87
Ti@Mg	3.1±0.1	3.8±0.2	1.9±0.2	2.0	0.59±0.04	0.66
Ti@Zn	3.1±0.1	4.1±0.2	2.3±0.2	2.1	0.67±0.03	0.68

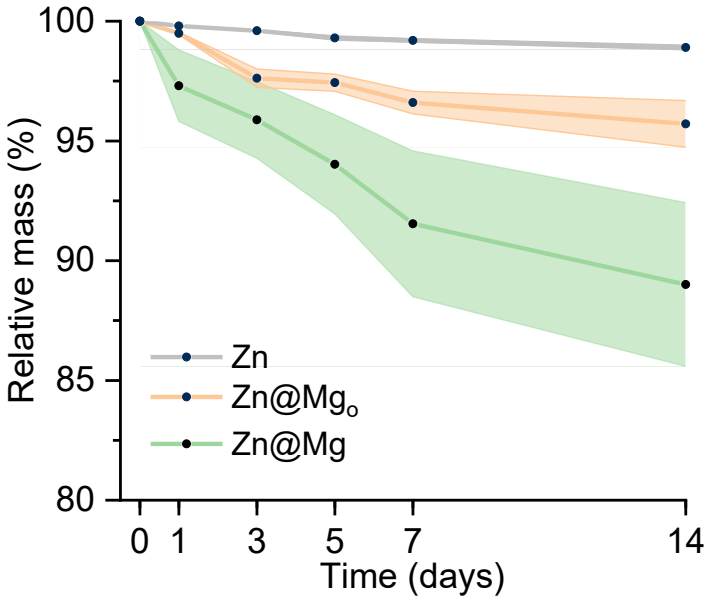

Fig. S6 *In vitro* degradation weight loss. Data are presented as mean ± SD.

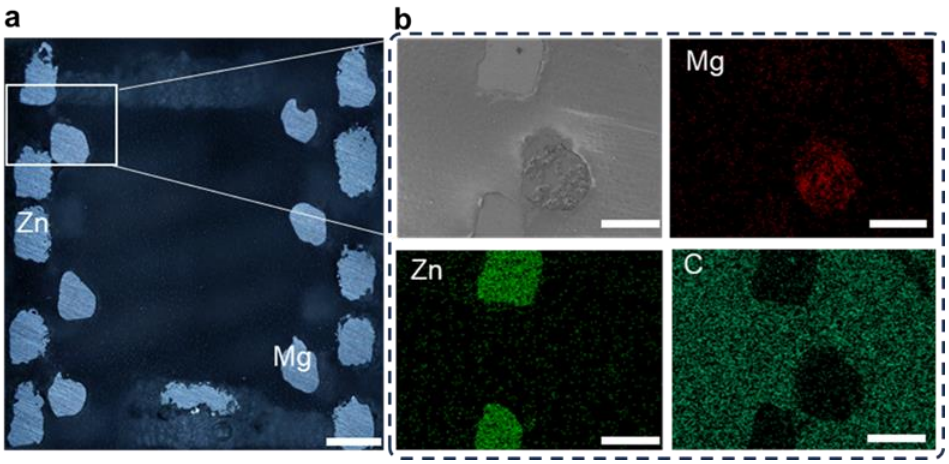

Fig. S7 EDS characterization of cross-sectional Zn@Mg.

Supplementary Note 3: Cell viability tests of stretching-type 4DAMS

Metal scaffolds are primarily utilized for bone implants and vascular stents in biomedical engineering. Osteoblasts and endothelial cells are two major effector cells during bone regeneration and vessel healing. The impact of Zn, Zn@Mg_o, and Zn@Mg extracts on the biocompatibility of Mouse-derived preosteoblasts (MC3T3-E1) and human umbilical vein endothelial cells (HUVECs) are presented in Fig. S8-S12. As shown in Fig. S8, inductively coupled plasma spectrometer (ICP) analysis of the 100% extracts showed that Zn@Mg had the highest concentration of Mg ions. Zn ion concentrations were similar in Zn@Mg and Zn@Mg_o, as the primary degradation occurred in the Mg component of both samples. The extracts provide insights into the degradation of different scaffolds and eliminate the effects of recovery force, offering a basis for the following in vivo studies on scaffold recovery and tissue repair.

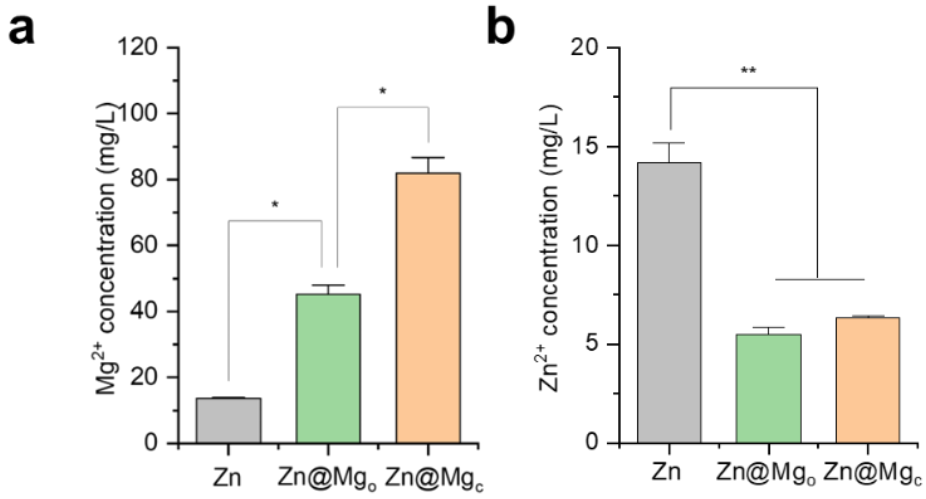

Fig. S8 Ionic concentrations in 100% extracts. a Mg^{2+}, **b** Zn^{2+}. *p < 0.05, **p < 0.01, ***p < 0.005. Data are presented as mean ± SD.

Zn@Mg and Zn@Mg_o significantly enhanced the proliferation of MC3T3-E1 cells and demonstrated superior cell spreading and proliferation compared to the Zn group as shown in Fig. S9. This effect persisted even after a fourfold dilution (25%) (Fig. S10). All undiluted extracts (100%) showed cytotoxicity after five days of culture. To assess the impact on osteogenic differentiation, MC3T3-E1 cells were cultured in osteogenic medium (CM) for 14 days with 50% concentration. ALP staining and activity results in Fig. 4c indicated a modest increase in ALP expression for Zn@Mg and Zn@Mg_o compared to Zn. Additionally, ARS staining revealed that Zn@Mg exhibited significantly larger and more numerous mineralized nodules than Zn@Mg_o and Zn, indicating higher calcium deposition efficiency by MC3T3-E1 cells. In short, the Zn@Mg 4DAMS, which releases more Mg ions than Zn@Mg_o, promotes calcium deposition in MC3T3-E1, but does not significantly enhance MC3T3-E1 cell proliferation.

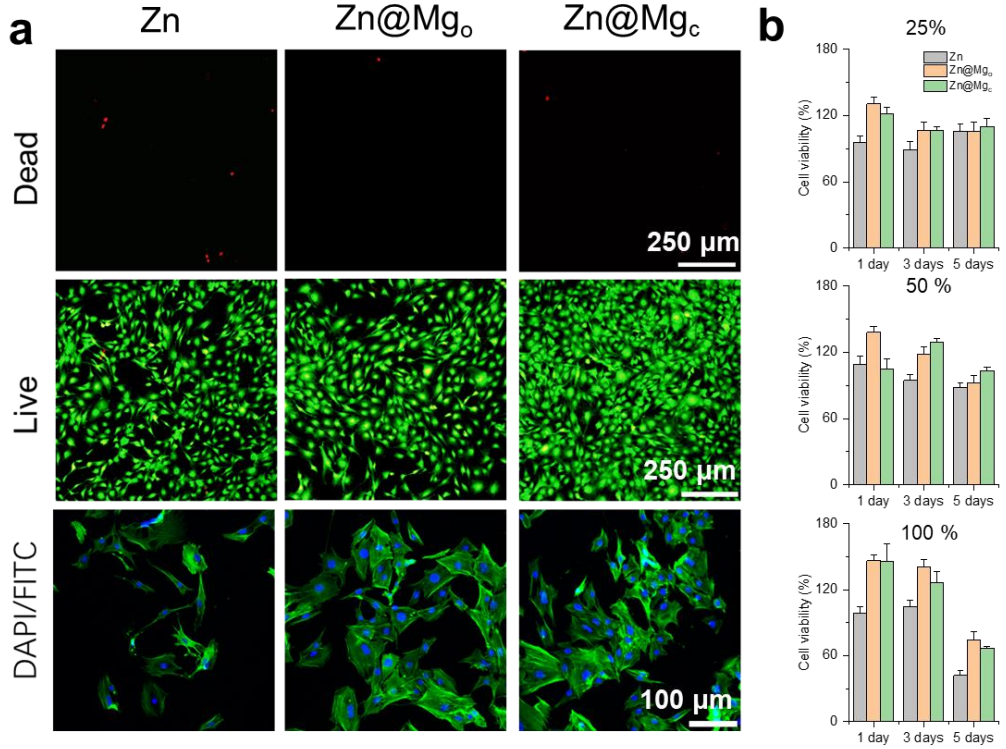

Fig. S9 MC3T3-E1 cell biocompatibility evaluation. a Live/dead staining and DAPI/FITC staining of MC3T3-E1 cells at 24 h in 50% extracts. **b** CCK-8 cell proliferation tests after culturing with 25%, 50% and 100% concentration of material extracts. Data are presented as mean ± SD.

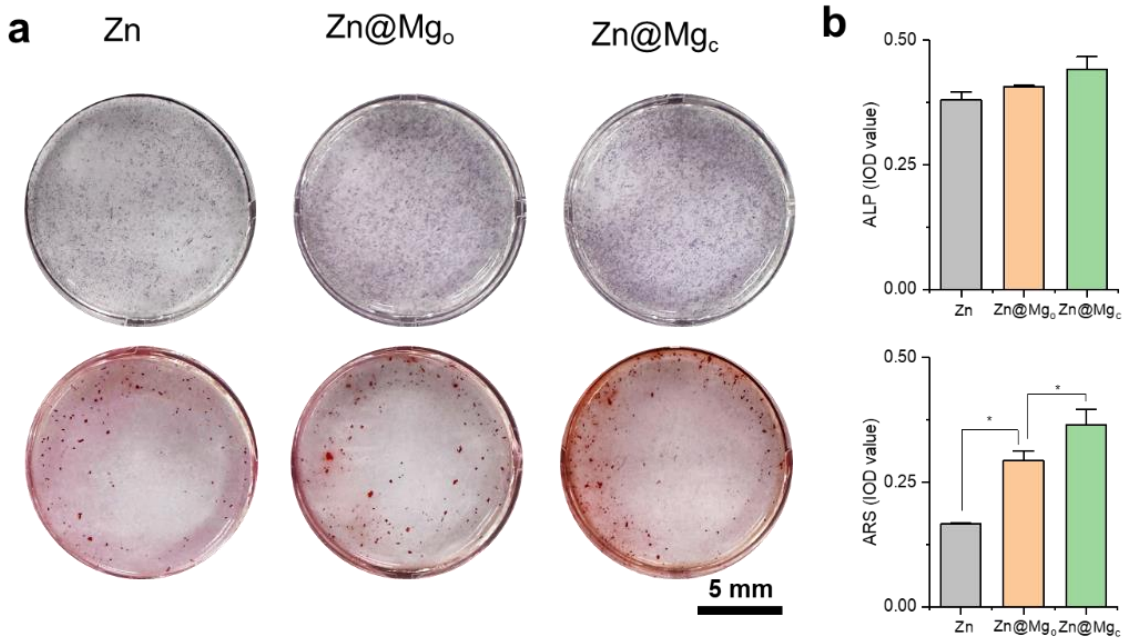

Fig. S10 MC3T3-E1 cell ontogenetic capability evaluation. a ALP staining and ARS staining of MC3T3-E1 after 14 days. **b** activity quantitative of the MC3T3-E1 (n = 5). ALP: alkaline phosphatase, ARS: Alizarin Red S. Data are presented as mean ± SD.

The cell viability test with HUVECs was further assessed using 100% concentration extracts. Live/dead staining showed good cell viability across all groups after 24 hours of culture, with Zn@Mg and Zn@Mg_o exhibiting better spindle-shaped cell morphology in Fig. S11a. Cell migration assays indicated that Zn@Mg and Zn@Mg_o significantly enhanced HUVECs migration compared to Zn, with only minor differences between the two (Fig. S11b). Proliferation tests (Fig. S12) revealed no significant differences among the three groups, suggesting that HUVECs proliferation is relatively insensitive to the concentrations of Mg and Zn ions.

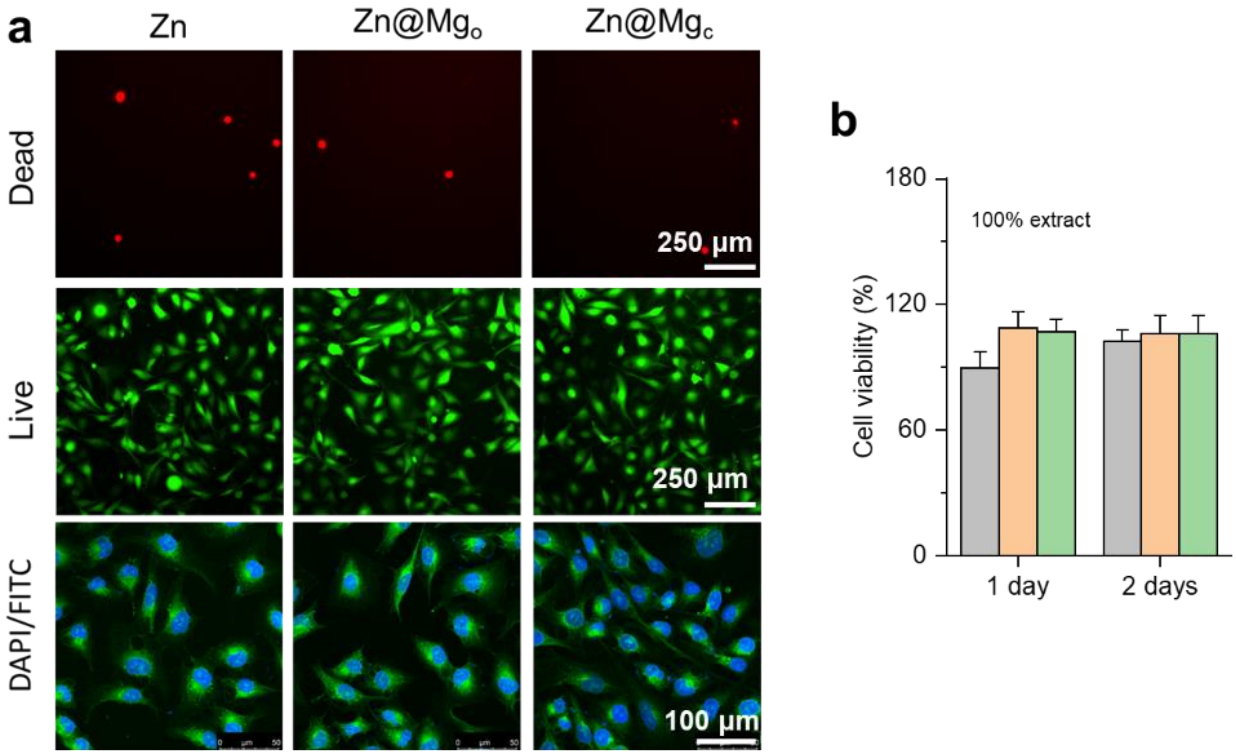

Fig. S11 HUVEC cell biocompatibility evaluation. a Live/dead staining and DAPI/FITC staining of HUVECs at 24 h in 100% extracts. **b** Cell viability, and proliferation after culturing with 100% concentration of material extracts. Data are presented as mean ± SD.

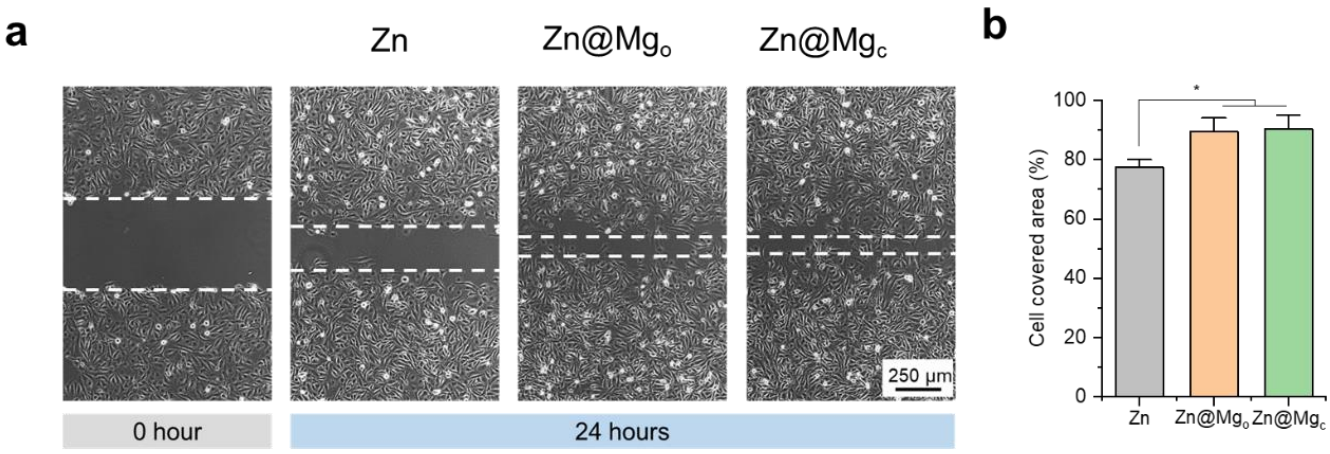

Fig. S12 HUVEC cell migration capability evaluation. a Cell migration after 24 h-culturing with 100% extracts. **b** Cell covered area. Data are presented as mean ± SD.

Supplementary Note 4: *In vivo* implantation of stretching-type 4DAMS

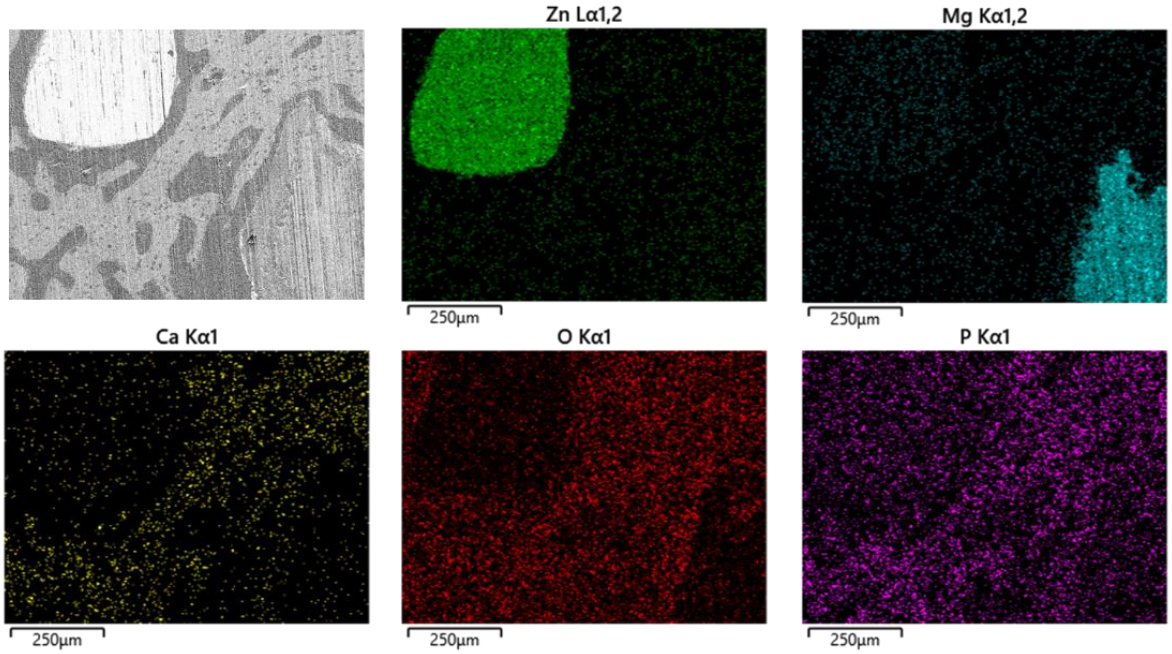

Fig. S13 SEM and EDS mapping of implanted Zn@Mg. The clearly visible irregularities in Mg morphology suggest ongoing degradation.

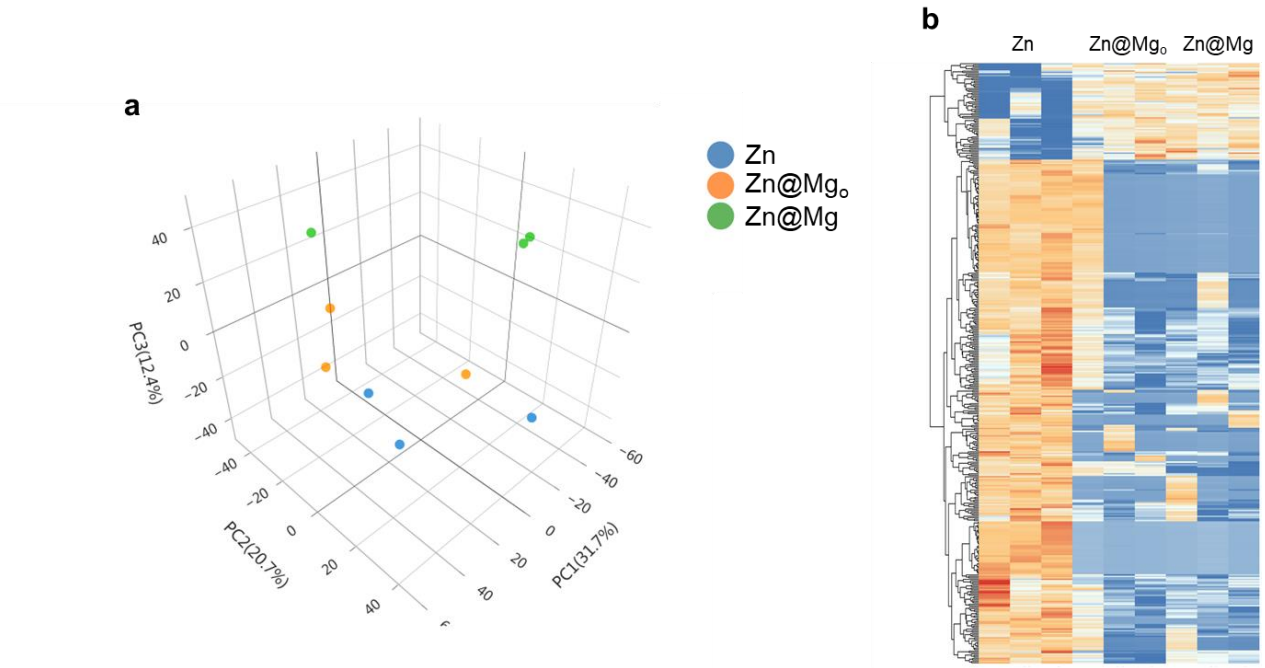

Fig. S14 Proteomic tests of Zn@Mg 4DAMS compared with Zn and Zn@Mg$_o$. a PCA plot. **b** Heatmap of differentially expressed proteins.

Supplementary Methods

Cell viability tests

MC3T3-E1 (NCACC SCSP-5218) and HUVECs (ATCC CRL-1730) were used to evaluate the impact of materials on cell biocompatibility. The MC3T3-E1 cells were cultured in MEM-α (Gibco) supplemented with 10% fetal bovine serum (FBS) and 1% antibiotic-antimycotic (100 U/mL penicillin and 100 μg/mL streptomycin) at 37 °C in a humidified atmosphere with 5% CO2. HUVECs were cultured with DMEM with 10% fetal bovine serum (FBS), 100 U/mL penicillin, and 100 μg/mL streptomycin at 37 °C in a humidified atmosphere of 5% CO_2.

Extracts of the scaffolds were prepared following the International Organization for Standardization method (ISO 10993-12). The scaffolds were first sterilized with UV light for 30 minutes on each side and then incubated in a medium with a volume-to-area ratio of 1.25 mL/cm² at 37°C for 24 hours. After incubation, the supernatants were collected and stored at 4°C. The concentrations of Zn and Mg ions in the alloys were measured using inductively coupled plasma (ICP) analysis.

Cell proliferation was studied using 100 μL cell suspension. Cell were seeded into a 96-well plate at a density of 5×10^4 cells/mL for each well and allowed to attach for 24 hours. The culture medium was then replaced with extracts of the materials, diluted from zero- to four-fold (100%-25% concentration), while culture medium and 10% dimethyl sulfoxide served as negative and positive controls, respectively. After incubating for 1, 3 and 5 days (MC3T3-E1) or 1 and 2 days (HUVECs), cell viability and proliferation were assessed using a cell viability kit (CCK-8, Dojindo, Kumamoto, Japan). Each group was measured in five duplicates.

For fluorescence microscopy (Olympus, Japan) observation, cells were stained following a Live/Dead staining procedure (Viability/Cytotoxicity Assay Kit for Animal Live & Dead Cells (Calcein, AM EthD-I)). For confocal (CLSM, Leica TCS SP5, Germany) visualization, 1 mg/mL DAPI and 1.0% v/v FITC–phalloidin (sigma) were used to stain the nuclei and actin, respectively.

To measure the cell migration, cells were seeded in a 6-well plate and cultured with normal medium for 48–72 h to reach confluency. A 10-μL lance tip was used to scratch along the line on the back side of the plate, with the tip kept vertical and not tilted. Then damaged cells were washed up with a PBS solution for three times. Serum-free medium containing the corresponding extracts was added and cultured for 0 and 24h, and then photographed.